# Effective Borehole Thermal Resistance of A Single U-Tube Ground Heat Exchanger

## Quan Liao , Chao Zhou , Wenzhi Cui & Tien-Chien Jen

# EFFECTIVE BOREHOLE THERMAL RESISTANCE OF A SINGLE U-TUBE GROUND HEAT EXCHANGER

## Quan Liao[1,2], Chao Zhou[2], Wenzhi Cui[1,2], and Tien-Chien Jen[3]

[1]*Key Laboratory of Low-Grade Energy Utilization Technologies and Systems (Chongqing University), Ministry of Education, Chongqing, P.R. China*
[2]*College of Power Engineering, Chongqing University, Chongqing, P.R. China*
[3]*Department of Mechanical Engineering, University of Wisconsin-Milwaukee, Milwaukee, Wisconsin, USA*

*The effective borehole thermal resistance of a vertical, single U-tube ground heat exchanger is numerically studied. The nonuniform temperature distributions along the perimeter of both borehole and outside diameter of two pipes are taken into account to evaluate effective borehole thermal resistance. A best-fit correlation for effective borehole thermal resistance is proposed, and the dimensionless borehole thermal resistances are compared between the present correlation and other available equations in the literature. It is found that the present correlation of effective borehole thermal resistance is more accurate than those of available formulas.*

## 1. INTRODUCTION

A ground-source heat pump (GSHP) uses the earth as a heat source or heat sink to extract or reject the thermal energy. Since the annual temperature fluctuation of soil under the ground is relatively small, the GSHP system has been recognized as one of the most energy-efficient systems for space heating and cooling in residential and commercial buildings. In a GSHP system, one of the most important components is the ground-coupled heat exchanger, through which thermal energy is exchanged between heat carrier fluid (i.e., water or water-antifreeze fluid) and soil. Since the ground heat exchanger is responsible for a major portion of the initial cost of the GSHP system, and the efficiency of this system depends on the performance of a ground heat exchanger, careful design of the ground heat exchanger is crucial for successful application of the GSHP system [1].

## NOMENCLATURE

| | | | |
|---|---|---|---|
| $D$ | diameter, m | $\delta$ | thickness of pipe, m |
| $k$ | thermal conductivity, W/m-K | | |
| $n$ | number of pipes | **Subscripts** | |
| $q$ | heat transfer rate per unit length, W/m | $b$ | borehole |
| $R$ | thermal resistance, m-K/W | $p$ | pipe |
| $S$ | shank spacing, m | $g$ | grout |
| $T$ | temperature, K | $s$ | soil |
| $\theta$ | dimensionless parameter of borehole geometry | $1b$ | pipe #1 to borehole |
| | | $2b$ | pipe #2 to borehole |
| $\sigma$ | dimensionless parameter of thermal properties between grout and soil | | |

For a typical single U-tube ground heat exchanger (as shown in Figure 1), a U-shape pipe is vertically and symmetrically inserted in a borehole and the gap between the pipes and borehole is filled by grout material. A heat carrier fluid is circulated in the U-shape pipe and heat is exchanged between carrier fluid and soil through pipes and grout within the borehole.

Since the effective borehole thermal resistance, which is defined as the thermal resistance between the outside diameter of pipes and borehole for a unit length of ground heat exchanger, plays a dominant role to size the ground heat exchanger, some analytical and numerical models were proposed to estimate it based on the 2-D heat conduction problem with different geometry parameters and thermal properties of soil and grout, as shown in Figure 2. The geometry parameters of the single U-tube ground heat exchanger could be described by borehole diameter $D_b$ outside diameter of pipe $D_p$ and shank spacing $S$. The thermal conductivities
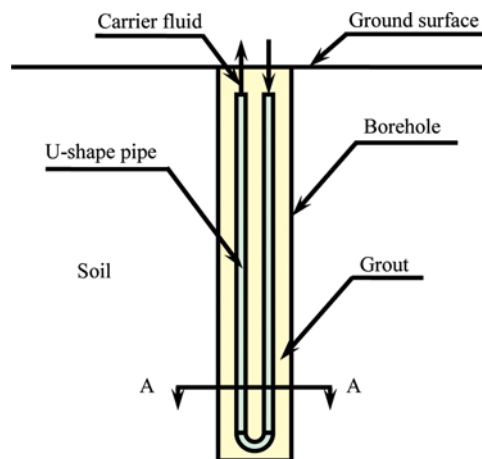


**Figure 1.** Schematic diagram of a typical single U-tube ground heat exchanger (color figure available online).
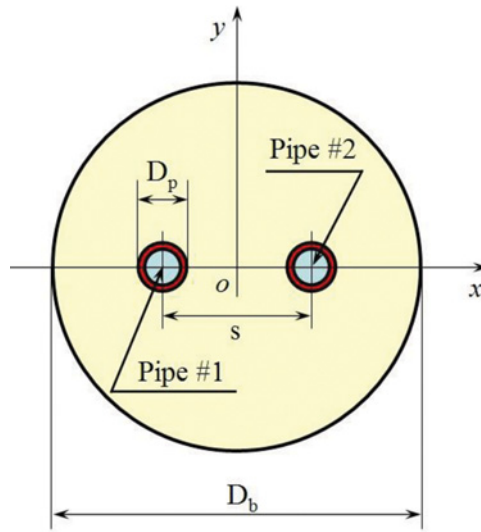
**Figure 2.** Schematic diagram of A-A cross-section view in Figure 1 (color figure available online).

of soil and grout are $k_s$ and $k_g$, respectively; therefore, four dimensionless variables of ground heat exchanger could be defined as follows:

$$\theta_1 = \frac{S}{D_b} \tag{1}$$

$$\theta_2 = \frac{D_b}{D_p} \tag{2}$$

$$\theta_3 = \frac{D_p}{2S} = \frac{1}{2\theta_1 \cdot \theta_2} \tag{3}$$

$$\sigma = \frac{k_g - k_s}{k_g + k_s} \tag{4}$$

Shonder and Beck [2] simplified the complicated geometry parameters of the ground heat exchanger and treated U-shape pipes as a single coaxial pipe with an equivalent diameter that has the same cross-section area as those of the U-shape pipes. Therefore, the complex geometry of borehole is represented as a coaxial pipe, and the effective borehole thermal resistance was given as follows.

$$R_b = \frac{1}{2\pi \cdot k_g} \ln\left(\frac{\theta_2}{\sqrt{n}}\right) \tag{5}$$

where $n$ is the number of pipes within the borehole, and $k_g$ is the thermal conductivity of grout material. Since this simple model neglects the thermal interference

between the pipes, the effective borehole thermal resistance of Eq. (5) is not the function of shank spacing, i.e., $S$.

Sharqawy et al. [3] developed a 2-D numerical model that assumes steady-state heat conduction within the borehole. The different geometry of the U-tube ground heat exchanger and the thermal property of grout were considered in the simulations. After numerous simulations were performed, a best-fit correlation was obtained for the effective borehole thermal resistance.

$$R_b = \frac{1}{2\pi \cdot k_g}[-1.49 \cdot \theta_1 + 0.656 \ln(\theta_2) + 0.436] \tag{6}$$

Although Sharqawy claimed that the accuracy of Eq. (6) to estimate effective borehole thermal resistance is better than other available formulas in the literature, Lamarche et al. [4] pointed out the boundary conditions (i.e., uniform temperature distributions for the borehole and outside diameter of pipes, respectively) adopted in the 2-D model by Sharqawy is *not* consistent with the real physical situation. An improved 2-D numerical model was developed and solved by using COMSOL$^{\text{TM}}$ finite element software. This improved 2-D model considers the soil surrounding the borehole region, and the distance between the inner and outer soil surfaces is much greater than the diameter of the borehole. Since the isothermal boundary conditions are imposed at the outside diameter of the pipes and soil outer surface, there is no more constrain for the temperature distribution along the perimeter of the borehole, and nonuniform temperature distribution on the borehole was observed. After comprehensive comparisons of borehole thermal resistance between the existing formulas and numerical simulation data, Lamarche concluded that the equation proposed by Bennet et al. [5] gives the best estimation for the borehole thermal resistance, and the root mean square error between the simulation data and the Bennet formula is less than 0.003. The equation of borehole thermal resistance proposed by Bennet et al. is as follows.

$$R_b = \frac{1}{4\pi \cdot k_g}\left[\ln\left(\frac{\theta_2}{2\theta_1\left(1-\theta_1^4\right)^{\sigma}}\right) - \frac{\theta_3^2 \cdot \left(1-\frac{4\sigma \cdot \theta_1^4}{1-\theta_1^4}\right)^2}{1+\theta_3^2 \cdot \left(1+\frac{16\sigma \cdot \theta_1^4}{\left(1-\theta_1^4\right)^2}\right)}\right] \tag{7}$$

where all the dimensionless parameters are defined in Eq. (1)–(4). $k_g$ and $k_s$ are thermal conductivities of grout and soil, respectively.

Although the improved 2-D model by Lamarche et al. considered the nonuniform temperature distribution on the borehole, the isothermal boundary conditions are still imposed at the outside diameter of the pipes. Unfortunately, in a real physical situation using a ground heat exchanger, not only is the temperature distribution at the borehole nonuniform, but the temperature at the outside diameter of the pipes is too. All these angular variations of temperature at the borehole and outside diameter of the pipes are due to the symmetrical arrangement of pipes, temperature differences of carrier fluid between pipes, and the thermal conductivities of pipe, grout, and soil. In order to consider the influence of nonuniform temperature at the outside diameter of pipes to the effective borehole thermal resistance, the thickness of pipes

are taken into account by a new 2-D numerical model in the present article, and the third kind of boundary conditions (i.e., the temperature of carrier fluid and heat transfer coefficient are given) are imposed at the inner diameter of the pipes.

After systematically selecting dimensionless geometrical variables and thermal properties of grout and soil in a ground heat exchanger, the new 2-D numerical model was solved by Fluent 6.3.26 software, and the effective borehole thermal resistances could be obtained based on the average temperatures of the outside diameter of the pipes and the average temperature of the borehole. Eventually, a new best-fit correlation for effective borehole thermal resistance is proposed by using the Nealder Mead method [6], and comprehensive comparisons between the present correlation and available formulas in the literature are presented here.

## 2. PHYSICAL AND MATHEMATICAL MODEL

In order to consider the nonuniform temperature distributions at the borehole and outside diameter of the pipes, a 2-D numerical model consisting of soil, grout, and thickness of pipes was developed. As shown in Figures 2 and 3, the geometry and meshes of this new model are presented, respectively.

In Table 1, the geometrical parameters and thermal properties of the numerical model are given as such: the outside diameter of soil ($D_{soil}$), diameter of borehole ($D_b$), outside diameter of pipe ($D_p$), shank spacing ($S$), thickness of pipes ($\delta$), and thermal conductivity of pipes ($k_{pipe}$). In a real U-shape pipe, since the minimum bending diameter is 1.5 times the outside diameter of the pipe, the range of shank spacing is between $1.5D_p$ and $D_b$-$D_p$.

To solve the above 2-D heat conduction problem, several assumptions were made.

• Steady-state 2-D heat conduction is assumed for this numerical model.
• The materials (including soil, grout, and pipes) are homogenous and all thermal properties are independent of temperature.
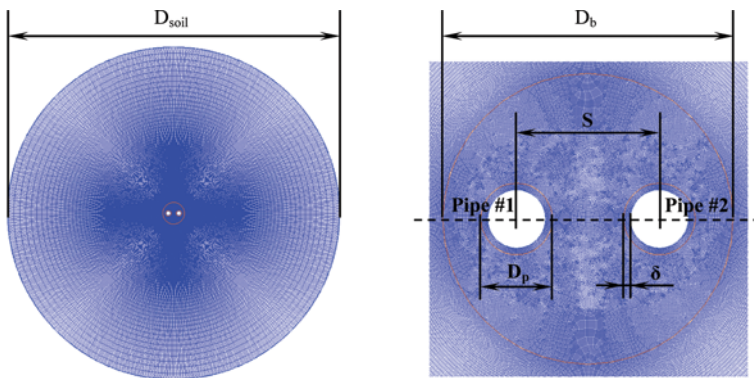


(a) Mesh of two pipes, borehole and soil   (b) Detailed mesh of borehole and two pipes

**Figure 3.** Computational domain and meshes in a new 2-D model (color figure available online).

**Table 1.** Range of parameters in the present 2-D numerical model

| $D_{soil}$ (m) | $D_b$ (m) | $D_p$ (m) | $S$ (m) | $\delta$ (m) | $k_{pipe}$ (W/m-K) |
|---|---|---|---|---|---|
| 4.0 | 0.13~0.2 | 0.025~0.065 | $1.5D_p$~$D_b$-$D_p$ | 0.003 | 0.44 |

Under the above assumptions, the governing equation of 2-D steady-state heat conduction in a Cartesian $x$-$y$ coordinate system could be written as follows.

$$\frac{\partial^2 T}{\partial x^2} + \frac{\partial^2 T}{\partial y^2} = 0 \tag{8}$$

The boundary conditions for the above-governing equation are: constant temperature is imposed at the outside diameter of soil, and the third kind of boundary condition (i.e., the carrier fluid temperature and heat transfer coefficient are given) is imposed at the inner surface of the pipes.

As shown in Figure 4, a four-thermal-resistance circuit can be developed to evaluate the effective borehole thermal resistance, i.e., $R_b$. Due to the symmetrical arrangement of the borehole, the thermal resistance $R_{1b}$ is equal to $R_{2b}$ and the effective borehole thermal resistance could be written as follows.

$$R_b = \frac{R_{1b}}{2} = \frac{R_{2b}}{2} = \frac{(T_{p1} + T_{p2}) - (T_{b1} + T_{b2})}{2 \cdot (q_1 + q_2)} \tag{9}$$

where $T_{p1}$ and $T_{p2}$ are the average temperatures at the outside diameter of pipe #1 and pipe #2, respectively. $T_{b1}$ and $T_{b2}$ are the average temperatures with half perimeter of the borehole, as shown in Figure 4. $q_1$ and $q_2$ are the rate of heat transfer from pipe #1 and pipe #2, respectively.
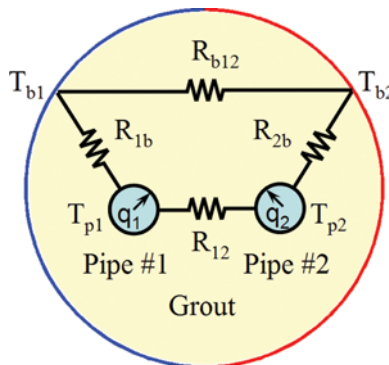


**Figure 4.** Diagram of a thermal resistance circuit for the borehole (color figure available online).

**Table 2.** Range of parameters in the validation numerical model

| $D_{soil}$ (m) | $D_p$ (m) | $D_b$ (m) | $S$ (m) | $k_s$ (W/m-K) | $k_g$ (W/m-K) |
|---|---|---|---|---|---|
| 4.0 | 0.025 | 0.125 | 0.05/0.0875 | 1.8 | 1.2~7.2 |

## 3. VALIDATION OF NUMERICAL METHOD

To validate the present numerical technique, Lamarche's 2-D numerical model was obtained by deleting the pipes in the present 2-D numerical model (as shown in Figure 3), and constant temperature boundary conditions were imposed at both the outside diameter of pipes and outer boundary of computational domain, respectively. In this validation numerical model, the geometrical parameters and thermal properties of soil and grout are given in Table 2.

When all of the parameters are set up, the numerical simulations of the validation model are carried out with different thermal conductivity of grout. As shown in Table 3 and Figure 5, the comparisons of dimensionless borehole thermal resistance between numerical simulation results in the validation model and Eq. (7) are presented. Table 3 and Figure 5 clearly show that the numerical simulation results agree very well with the results of Bennet et al., i.e., Eq. (7). The maximum relative error between them is less than 0.2%, which is consistent with the conclusions of Lamarche et al. [4]. Therefore, it could be reasonably believed that the present numerical technique is reliable and all simulation results based on this technique are valid.

**Table 3.** Comparisons of dimensionless borehole thermal resistance between the validation model and Bennet et al. (Eq. (7))

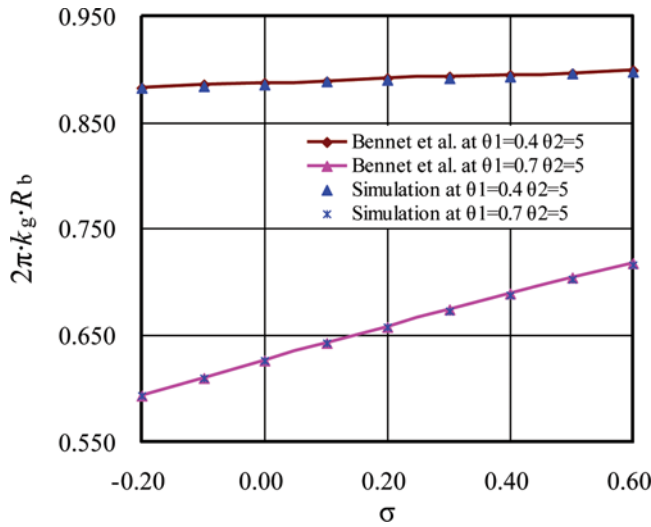| $\theta_1$ | $\sigma$ | Simulation results | Bennet et al. Eq. (7) | Relative error (%) |
|---|---|---|---|---|
| 0.4 | −0.2 | 0.882148 | 0.882880 | 0.08% |
|  | −0.1 | 0.884111 | 0.884884 | 0.09% |
|  | 0 | 0.886056 | 0.886879 | 0.09% |
|  | 0.1 | 0.887992 | 0.888863 | 0.10% |
|  | 0.2 | 0.889915 | 0.890838 | 0.10% |
|  | 0.3 | 0.891833 | 0.892803 | 0.11% |
|  | 0.4 | 0.893735 | 0.894758 | 0.11% |
|  | 0.5 | 0.895630 | 0.896703 | 0.12% |
|  | 0.6 | 0.897517 | 0.898638 | 0.12% |
| 0.7 | −0.2 | 0.592905 | 0.592903 | 0.00% |
|  | −0.1 | 0.609874 | 0.609896 | 0.00% |
|  | 0 | 0.626385 | 0.626483 | 0.02% |
|  | 0.1 | 0.642464 | 0.642679 | 0.03% |
|  | 0.2 | 0.658125 | 0.658501 | 0.06% |
|  | 0.3 | 0.673386 | 0.673962 | 0.09% |
|  | 0.4 | 0.688277 | 0.689075 | 0.12% |
|  | 0.5 | 0.702796 | 0.703855 | 0.15% |
|  | 0.6 | 0.716974 | 0.718312 | 0.19% |

**Figure 5.** Comparisons of dimensionless borehole thermal resistance between simulation results and Bennet et al. (Eq. (7)) (color figure available online).

## 4. RESULTS AND DISCUSSION

To demonstrate the nonuniform temperature distributions at the borehole and outside diameter of the pipes, the 2-D numerical model with 4.0 m outside diameter of the soil, 0.153 m borehole diameter, 0.06 m outside diameter of the pipes, 0.09 m shank spacing, and 0.003 m thickness of the pipes was numerically solved by Fluent 6.3.26 with 300.0 K constant temperature at the outside diameter of soil, 325.0 K fluid temperature for pipe #1, 320.0 K fluid temperature for pipe #2, 4000.0 W/m$^2$-K heat transfer coefficient for the inner surface of pipes #1 and #2, 0.44 W/m-K thermal conductivity for the pipes, 1.8 W/m-K thermal conductivity for the soil, and 2.0 W/m-K thermal conductivity for the grout. As shown in Figures 6 and 7, the temperature distributions along the angular direction of the borehole and outside diameter of the pipes are presented. These two figures clearly show the temperature distributions at both the borehole and outside diameter of the pipes are indeed *not* uniform.

Since the numerical technique in this article has been verified, the simulations of the new 2-D model for a ground heat exchanger were systematically carried out for different combinations of dimensionless parameters of $\theta_1$, $\theta_2$, and $\sigma$. At the end of each simulation, the effective borehole thermal resistance, i.e., $R_b$, was obtained by using Eq. (9). In this article, 744 numerical simulations were systematically conducted and all the data of $R_b$, $\theta_1$, $\theta_2$, and $\sigma$ were collected. The Nealder Mead method was adopted to obtain the relationship between these primary simulation data sets of $R_b$, $\theta_1$, $\theta_2$, and $\sigma$. Eventually, a best-fit correlation for the effective borehole thermal resistance, i.e., $R_b$, is obtained.
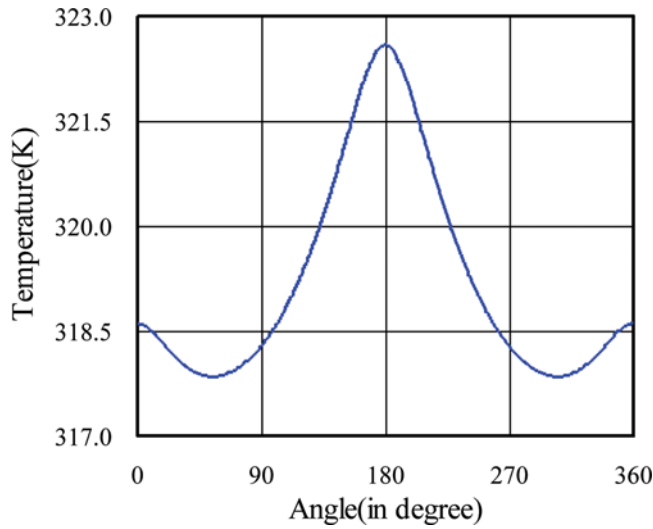
**Figure 6.** Temperature distribution along the angular direction of the borehole (color figure available online).

$$R_b = \frac{1}{2\pi \cdot k_g}\left[-0.50125\ln(\theta_1) + 0.51248\ln(\theta_2) + 0.51057\sigma \cdot \ln\left(\frac{1}{1-\theta_1^4}\right) - 0.36925\right]$$

(10)

According to the numerical simulation data, the above-correlation has relative errors of maximum 3.08% and minimum −1.70%, and the root mean square error is
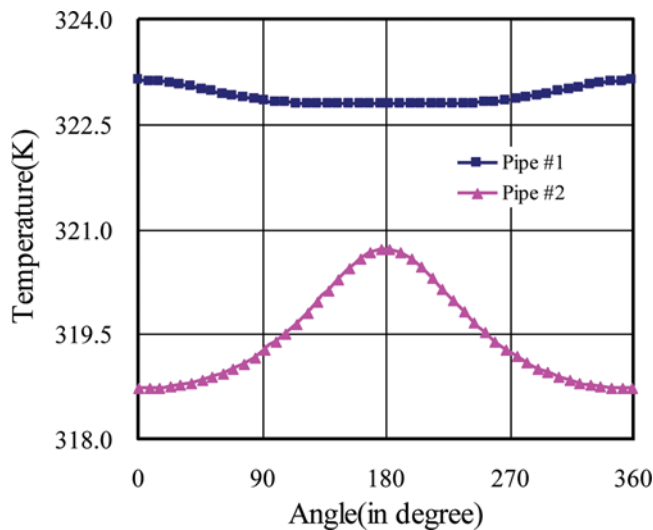


**Figure 7.** Temperature distributions along the angular direction of the outside diameter of pipes #1 and #2 (color figure available online).
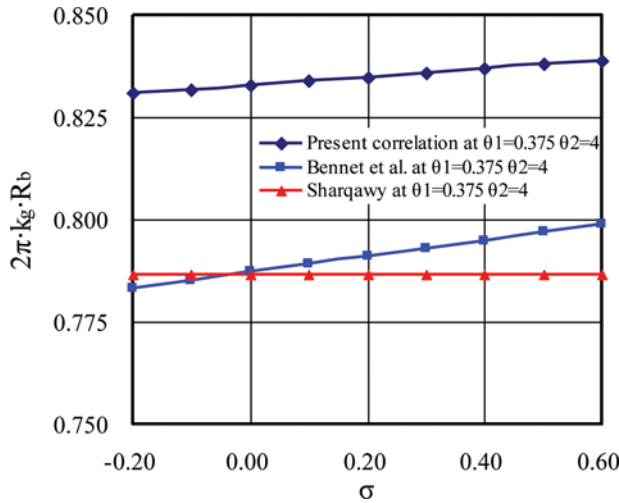
**Figure 8.** Comparisons of dimensionless borehole thermal resistance at $\theta_1 = 0.375$ and $\theta_2 = 4$ when $\sigma$ is between $-0.2$ and $0.6$ (color figure available online).

3.06E-4 for all 744 data sets. Therefore, Eq. (10) is relatively accurate enough to estimate the effective borehole thermal resistance within the range of dimensionless parameters $-0.2 \leq \sigma \leq 0.6$, $-0.214 \leq \theta_1 \leq 0.85$, and $2.5 \leq \theta_2 \leq 7.0$.

To show the differences between the present correlation and available formulas for estimating effective borehole thermal resistance, the comparisons between the present correlation, the Bennet equation, i.e., Eq. (7), and the Sharqawy formula, i.e., Eq. (6), are presented with different combinations of dimensionless parameters $\theta_1$, $\theta_2$, and $\sigma$.
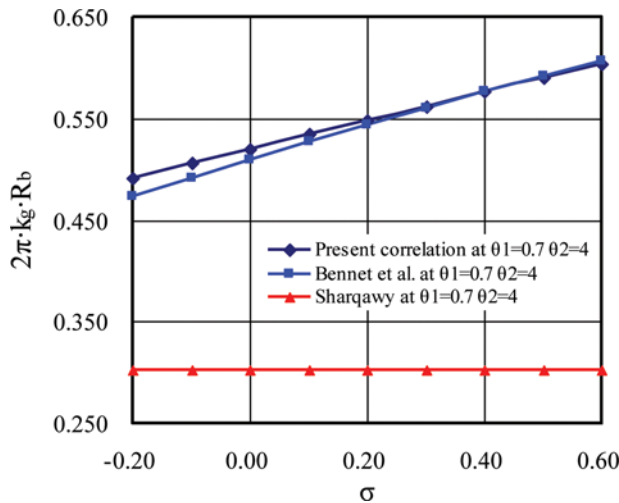


**Figure 9.** Comparisons of dimensionless borehole thermal resistance at $\theta_1 = 0.7$ and $\theta_2 = 4$ when $\sigma$ is between $-0.2$ and $0.6$ (color figure available online).
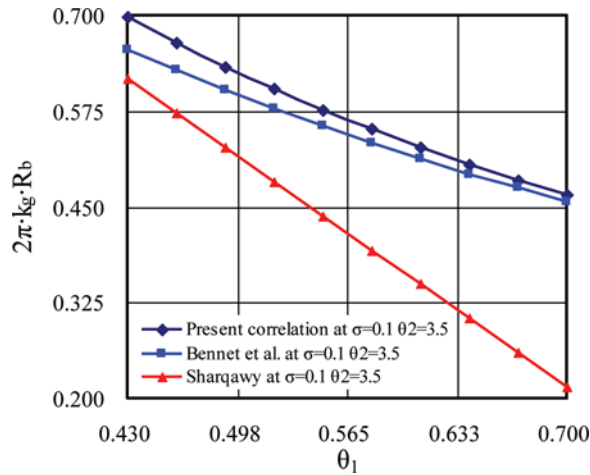
**Figure 10.** Comparisons of dimensionless borehole thermal resistance at $\sigma = 0.1$ and $\theta_2 = 3.5$ when $\theta_1$ is between 0.43 and 0.7 (color figure available online).

As shown in Figures 8 and 9, the relationships between $2\pi \cdot k_g \cdot R_b$ and $\sigma$ are presented at the condition of $\theta_2 = 4$, $\theta_1 = 0.375$, or $\theta_1 = 0.7$. Since the correlation of Sharqawy is not the function of $\sigma$, the dimensionless thermal resistance of Eq. (6) is independent of thermal conductivity of the soil. Comparing Figures 8 and 9, one could find the differences of $2\pi \cdot k_g \cdot R_b$ between the present correlation, and Eq. (7) decrease as the dimensionless parameters $\theta_1$ and $\sigma$ increase. This could be explained as follows. On the one hand, with the increase of $\theta_1$, the distance between the two pipes increases for a given borehole diameter, and the influence of temperature differences between two carrier fluids in the pipes to the nonuniform
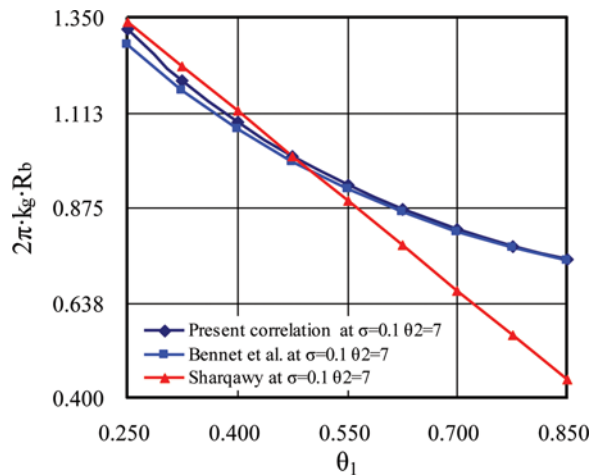


**Figure 11.** Comparisons of dimensionless borehole thermal resistance at $\sigma = 0.1$ and $\theta_2 = 7.0$ when $\theta_1$ is between 0.25 and 0.85 (color figure available online).
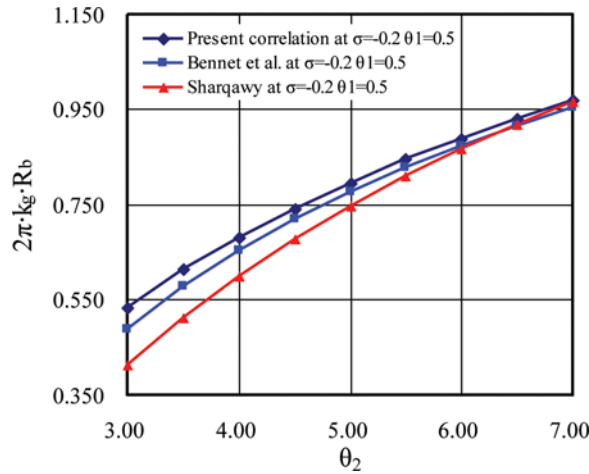
**Figure 12.** Comparisons of dimensionless borehole thermal resistance at $\sigma = -0.2$ and $\theta_1 = 0.5$ when $\theta_2$ is between 3.0 and 7.0 (color figure available online).

temperature distribution at the outside diameter of the pipes decreases. Therefore, the temperature distributions at the outside diameter of the pipes become uniform, and the differences between the third kind of boundary condition in the present model and the isothermal boundary condition in Lamarche's model decrease. On the other hand, as $\sigma$ increases, the thermal conductivity of soil decreases for a given grout thermal conductivity and the total rate of heat transfer from borehole to soil decreases. Therefore, the temperature distributions at the outside diameter of the pipes become uniform and the difference of the boundary condition between the present model and Lamarche's model decreases.
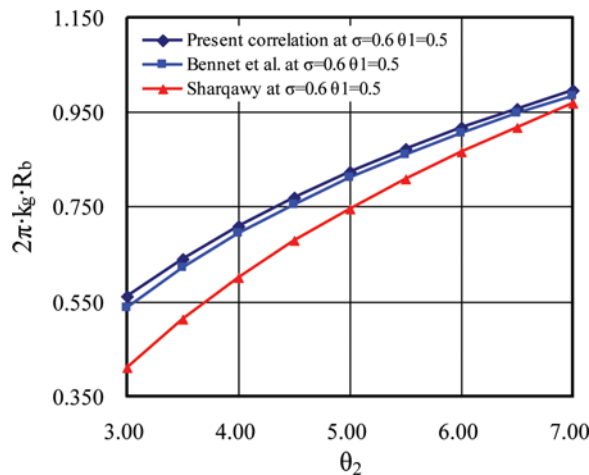


**Figure 13.** Comparisons of dimensionless borehole thermal resistance at $\sigma = 0.6$ and $\theta_1 = 0.5$ when $\theta_2$ is between 3.0 and 7.0 (color figure available online).

In Figures 10 and 11, the relationships between $2\pi \cdot k_g \cdot R_b$ and $\theta_1$ are presented at the condition of $\sigma = 0.1$, $\theta_2 = 3.5$, or $\theta_2 = 7.0$. From these two figures, it can be seen that these three correlations have the similar trend as $\theta_1$ increases, i.e., the dimensionless effective borehole thermal resistance of these three correlations decreases with an increase of $\theta_1$; however, the differences between the present correlation (or Bennet equation) and the Sharqawy formula increase as $\theta_1$ increases because the non-uniform temperature distribution at both the outside diameter of the pipes and the borehole become worse as the dimensionless parameter $\theta_1$ increases. On the other hand, the change of differences between the present correlation and the Bennet equation in Figures 10 and 11 decreases in terms of $2\pi \cdot k_g \cdot R_b$ when $\theta_1$ or $\theta_2$ increases. The same reasons adopted in Figures 8 and 9 could be explained for the changes of $2\pi \cdot k_g \cdot R_b$ versus $\theta_1$ in Figures 10 and 11.

As shown in Figures 12 and 13, the relationships between $2\pi \cdot k_g \cdot R_b$ and $\theta_2$ are presented at the condition of $\theta_1 = 0.5$, $\sigma = -0.2$, or $\sigma = 0.6$. From these two figures, we clearly see these three correlations have a similar trend of $2\pi \cdot k_g \cdot R_b$ versus $\theta_2$ at different values of $\sigma$ when $\theta_2$ increases, i.e., the dimensionless borehole thermal resistance gradually increases for a given $\sigma$; however, comparing these two figures, the influence of $\sigma$ to the value of $2\pi \cdot k_g \cdot R_b$ is much smaller than that of $\theta_2$. On the other hand, these two figures clearly show that the value of $2\pi \cdot k_g \cdot R_b$ in the present correlation is always higher than that of the Bennet equation and/or Sharqawy formula due to the difference in boundary conditions at the outside diameter of the pipes and the borehole for these three models.

## 5. CONCLUSION

A 2-D numerical model of a ground heat exchanger has been developed and solved. A best-fit correlation of borehole thermal resistance is proposed based on the systematical arrangement of 744 numerical simulations. The comparisons between the present correlation, Bennet equation, and Sharqawy formula are comprehensively presented here. Based on these comparisons, the following conclusions can be drawn.

- The temperature distributions at both the borehole and outside diameter of the pipes are *not* uniform, and are the functions of geometrical parameters (i.e., $\theta_1$ and $\theta_2$) and thermal properties of grout and soil (i.e., $\sigma$).
- The present correlation has similar relationships between $2\pi \cdot k_g \cdot R_b$ and $\sigma$, $\theta_1$, and $\theta_2$ as those of the Bennet equation and Sharqawy formula.
- The borehole thermal resistance of the present correlation is more accurate, and the values of $R_b$ are higher than those of the Bennet equation and Sharqawy formula under the same conditions.

## REFERENCES

1. J. D. Spitler GLHEPRO—A Design Tool for Commercial Building Ground Loop Heat Exchanger, *Proc. of the 4th Int. Conf. on Heat Pumps in Cold Climates*, Aylmer, QC, Canada, pp. 1–16, 2000.

2. J. A. Shonder and J. V. Beck, Field Test of a New Method for Determining Soil Formation Thermal Conductivity and Borehole Resistance, *ASHRAE Trans.*, vol. 106, pp. 843–850, 1999.
3. M. H. Sharqawy, E. M. Mokheimer, and H. M. Badr, Effective Pipe-to-Borehole Thermal Resistance for Vertical Ground Heat Exchangers, *Geothermics*, vol. 38, pp. 271–277, 2009.
4. L. Lamarche, S. Kajl, and B. Beauchamp, A Review of Methods to Evaluate Borehole Thermal Resistances in Geothermal Heat-Pump Systems, *Geothermics*, vol. 39, pp. 187–200, 2010.
5. J. Bennet, J. Claesson, and G. Hellstrom, Multipole Method to Compute the Conductive Heat Transfer to and Between Pipes in a Composite Clylinder, *Notes on Heat Transfer*, vol. 3. Department of Building Physics, Lund Institute of Technology, Lund, Sweden, 1987.
6. M. J. D. Powell, On Search Directions for Minimization Algorithms, *Mathematical Programming*, 4th edition, pp. 193–201, 1973.